PNAS RESEARCH ARTICLE | DEVELOPMENTAL BIOLOGY

Cis-inhibition suppresses basal Notch signaling during sensory organ precursor selection

Tobias Troost[a,1], Udi Binshtok[b,1], David Sprinzak[b,2], and Thomas Klein[a,2]

Edited by Hugo Bellen, Baylor College of Medicine, Houston, TX; received September 20, 2022; accepted March 29, 2023

The emergence of the sensory organ precursor (SOP) from an equivalence group in *Drosophila* is a paradigm for studying single-cell fate specification through Notch-mediated lateral inhibition. Yet, it remains unclear how only a single SOP is selected from a relatively large group of cells. We show here that a critical aspect of SOP selection is controlled by cis-inhibition (CI), whereby the Notch ligands, Delta (Dl), cis-inhibit Notch receptors in the same cell. Based on the observation that the mammalian ligand Dl-like 1 cannot cis-inhibit Notch in *Drosophila*, we probe the role of CI in vivo. We develop a mathematical model for SOP selection where Dl activity is independently regulated by the ubiquitin ligases Neuralized and Mindbomb1. We show theoretically and experimentally that Mindbomb1 induces basal Notch activity, which is suppressed by CI. Our results highlight the trade-off between basal Notch activity and CI as a mechanism for singling out a SOP from a large equivalence group.

neurogenesis | Notch signaling | neural precursor selection | cis-inhibition | Delta-like-1

Significance

How a cell fate is imposed onto a single cell in a developing organism is a fundamental question of development. Focusing on the classical model of the sensory organ precursor cell (SOP) in *Drosophila*, we combine experiments and modeling to identify how a single SOP is selected from a group of equivalent proneural cells. We identified a two-step mechanism that relies on cis-inhibitory interactions between the Notch receptor and ligands. First, a small subgroup of cells is initially defined, from which a single SOP is subsequently selected. The role of cis-inhibitory interactions in selecting a single cell is likely relevant to many other developmental processes.

The Notch signaling pathway is conserved across all metazoans and has been linked to numerous developmental, homoeostatic, and disease-related processes (1). In *Drosophila*, signaling is initiated by binding of one of its two Notch ligands, Delta (Dl) or Serrate (Ser), to the Notch receptor. The binding triggers the release of the Notch intracellular domain (NICD) into the cytosol, from which it is transported into the nucleus, where it forms a transcriptional activator complex with the Centromer Binding Factor 1/Suppressor of Hairless/Lin-12 and Glp-1 phenotype 2 (CBF/Su(H)/Lag2) (CSL) transcription factor (2). A key requirement for the activation of the pathway is the endocytosis of the Notch ligands. It is initiated by ubiquitylating the intracellular domain of the ligands by two E3 ligases, Mindbomb1 (Mib1) and Neuralized (Neur).

An important posttranslational regulation mode of Notch signaling is through *cis*-inhibition (CI), whereby Notch ligands bind and inhibit Notch receptors in the same cell [(3–5), reviewed in ref. 6]. CI was shown to play a role during several developmental processes in *Drosophila* including the wing and the notum (7). Despite its importance, the functional roles of CI are not well understood since it is hard to tease apart the cis- and trans-activities of the ligands in in vivo settings.

A classical, extensively studied, patterning process mediated by Notch signaling is the selection of sensory organ precursor cells (SOP) of the sensory bristle from an equivalence group, termed the proneural cluster (PNC). The PNCs in the notum of the fly are defined by the expression of the proneural bHLH transcription factors Achaete (Ac) and Scute (Sc) (typically lumped together and denoted as Ac/Sc) (8). Their expression imposes an undecided proneural state to the cells from which they can progress to develop into SOPs or regress to the default epidermoblast state. Within a given PNC, a defined number of cells (1 or 2) eventually adopt the SOP fate. They are selected by the activity of the Notch pathway in a process termed lateral inhibition. According to the prevailing lateral inhibition model, SOP selection occurs through an intercellular transcriptional feedback (TFB) mechanism, termed here the TFB model (9). In the TFB model, Ac/Sc activate the expression of Dl, which activates the Notch pathway in its surrounding cells. Notch activity in each cell suppresses the expression of proneural genes and, hence, also of Dl. This feedback mechanism can amplify small initial differences in Ac/Sc expression and generates an all-or-none switch where one cell expresses high levels of proneural activity and becomes the SOP, whereas its neighbors switch to the epidermoblast fate.

Recent work provided strong evidence against the TFB model. Using the Mosaic Analysis with a Repressible Cell Marker (MARCM) clone technique, a *Dl/Ser* double-mutant PNC that also expressed either Dl or Ser at a uniform level in all mutant cells was generated (10). Surprisingly, the selection of the SOP proceeded normally, although the transcription of Dl was uncoupled from the proneural activity. These data suggest that differential expression of Dl, a crucial element in the TFB model, is dispensable for SOP selection. In line with this conclusion is the observation that the overall expression of Dl appears to be unchanged

Author affiliations: [a]Institut fuer Genetik, Heinrich-Heine-Universitaet Duesseldorf 40225 Duesseldorf, Germany; and [b]School of Neurobiology, Biochemistry, and Biophysics, The George S. Wise Faculty of Life Sciences, Tel Aviv University, Tel Aviv 69978, Israel

Author contributions: U.B., D.S., and T.K. designed research; T.T. and U.B. performed research; T.T., U.B., D.S., and T.K. analyzed data; and T.T., U.B., D.S., and T.K. wrote the paper.

The authors declare no competing interest.

This article is a PNAS Direct Submission.

[1]T.T. and U.B. contributed equally to this work.

[2]To whom correspondence may be addressed. Email: davidsp@tauex.tau.ac.il or thomas.klein@hhu.de.

This article contains supporting information online at https://www.pnas.org/lookup/suppl/doi:10.1073/pnas.2214535120/-/DCSupplemental.

Published May 30, 2023.

in *ac/sc* mutants (11, 12). Moreover, the TFB model cannot explain how the SOP, via a short-range signaling pathway (Notch), inhibits cells in the PNC that are not in direct contact with it. Overall, these observations raise significant questions on the mechanism underlying SOP selection and call for alternative models.

Theoretical analyses of the TFB model show that CI could play an important role during SOP selection by enhancing the fidelity and speed of the selection process, thereby generating a sharp switch between signal-receiving and -sending states (13–16). This is because an imbalance between Notch receptors and ligands at the cell surface can lead to a strong suppression of either the receptors or ligands, depending on the ratio between them. However, while CI has been identified as a regulatory mode during several developmental processes, experimental evidence for its requirement for SOP selection is missing.

We recently reexamined the formation of the SOP of the large mechanosensory bristle, the macrochaeta (12). We found that three main factors regulate SOP selection: i) The expression profiles of proneural genes exhibit broad peaks of expression that center around the future SOP. ii) There is a basal Notch activity within the entire notum driven by a combination of Mib1 activity and ubiquitin-independent activity. iii) The combination between basal Notch activity and the proneural expression peaks defines a subgroup within the PNC from which the SOP is selected in a Neur-dependent manner (via lateral inhibition). These observations suggest a picture where Notch has two distinct roles: to suppress differentiation across the notum and to generate lateral inhibition within a small subgroup of the PNC. Moreover, it suggests that SOP selection is mediated by regulation of Dl activity rather than transcriptional regulation of Dl. Since in the TFB model the suggested role of CI during lateral inhibition is based on the feedback on Dl expression, it is unclear whether and how it affects SOP selection within this picture.

Here, we use a combination of modeling and experiments to elucidate the role of CI during the selection process of the SOP. We developed a mathematical model termed the two-channel SOP (TCS) model that explicitly incorporates regulation of Notch-ligand activity by Mib1 and Neur and accounts for CI between receptors and ligands. Using Dll1, which is CI-deficient in *Drosophila*, we experimentally test the prediction of the TCS model. We identify a trade-off between the strength of CI and basal ligand activity mediated by Mib1, whereby reducing (strengthening) CI can be compensated by reducing (strengthening) basal ligand activity. Overall, our results provide evidence that CI is required for the selection of the SOP and provide a model for the SOP selection.

Results

Development of a Mathematical Model of SOP Selection. To get a better understanding of the SOP selection, we developed a mathematical model, termed the TCS model, that considers four coupled regulatory modules (Fig. 1*A*): ubiquitylation, trans-activation, CI, and transcriptional regulation. The ubiquitylation module is characterized by two parallel channels associated with the two E3 ubiquitin ligases of Dl, Neur and Mib1. The essential difference between the channels is that the Neur-mediated activation of Dl is regulated by Notch signaling, while the Mib1-mediated activation of Dl is not. The unregulated channel mediated by Mib1 leads to basal mutual inhibition normally preventing cells from differentiating into the SOP fate.

The trans-activation and CI modules describe the interactions between Notch receptors and ligands in trans- and in cis-, leading to activation and inhibition of Notch signaling, respectively. We assume that trans-activation occurs only from ubiquitylated ligands, while CI can occur between all ligand forms (16). We note that although residual signaling of Dl that is independent of Mib1 and Neur has been observed (17), we neglect this contribution here for simplicity.

Finally, the transcriptional regulation module describes the relation between Notch signaling, Ac/Sc levels, and Neur. Based on the known regulatory relations, we assume that Notch signaling activates E(spl) that suppresses Ac/Sc (18), which in turn activates Neur. We model the set of regulatory processes shown in Fig. 1*A* by a set of differential equations for the variables associated with the protein concentrations (as previously described in refs. 16 and 19; see *Materials and Methods*). These equations are then solved numerically and simulated on cells arranged in a 2D hexagonal lattice (Fig. 1 *B* and *C* and *SI Appendix*, Fig. S1). Critical parameters of the system are the levels of the proneural proteins Ac and Sc. The expression levels of Ac/Sc are known to be high within the PNC and low outside the PNC (12, 20, 21). In order to determine the parameter set and initial conditions in our simulations, we initially modeled situations with either uniformly low or uniformly high Ac/Sc expression levels (*SI Appendix*, Fig. S1 *A* and *A′*). At uniformly low Ac/Sc levels, Mib1-mediated activity induces basal Notch signaling that indirectly suppresses Neur and, thus, SOPs cannot develop (*SI Appendix*, Fig. S1*A*). In contrast, at uniformly high Ac/Sc levels, a salt-and-pepper-like pattern of SOPs emerges (red cells in *SI Appendix*, Fig. S1*A′*), typical for the Notch-mediated lateral inhibition process (9). We note, though, that unlike standard models of lateral inhibition, the feedback here is not through regulating Dl expression levels (which remain constant) but rather by regulating Dl activity (by regulating Neur expression levels). Thus, the model is consistent with the experimental observation that selection of SOP is normal, even when Dl is expressed under a constitutively active promoter (10).

We next wanted to simulate the situation where a PNC is defined. Experimental observations show that Ac/Sc activity is high at the center of the PNC and decays away from it (i.e., there is a prepattern of Ac/Sc) (12, 22). We therefore assumed that the Ac/Sc-expression rate exhibits a decaying radial profile (Gaussian) (*SI Appendix*, Fig. S1 *B* and *B′*). The length scale of the decaying gradient is on the order of one cell diameter, consistent with observed PNC length scales. The profile of the Ac/Sc gradient is chosen such that a subgroup within the PNC, called the Neur group, accumulates high enough levels of Ac/Sc in order to participate in the selection of SOP via lateral inhibition. Naturally, the gradient also creates a bias such that the central cell is selected as SOP from the Neur group, as it has the highest initial level of Ac/Sc (12, 22). By tuning the parameters controlling the Ac/Sc expression profile and the mutual inhibition (basal signal), the TCS model results in a situation where only one SOP is selected from the Neur group (Fig. 1*B*). Thus, the TCS model is able to capture the wild-type (WT) case where a single SOP is selected from the PNC. In the coming sections, we show that the TCS model captures the previously observed mutant behaviors as well as generates predictions that are tested experimentally.

The TCS Model Predicts That CI Is Required for SOP Selection. We next tested whether we can generate a prediction about the role of CI during SOP selection. To test the role of CI in SOP selection, we ran a simulation of the TCS model where the CI rate is set to zero, but all other parameters remain fixed. This simulation shows a complete suppression of SOP selection (Fig. 1*C*). The suppression occurs due to high basal Notch activity in all cells caused by the reduction in CI (see the green line in Fig. 1 *B* and *C*). Thus, the TCS model predicts that CI is required for SOP selection as it reduces basal Notch activity.

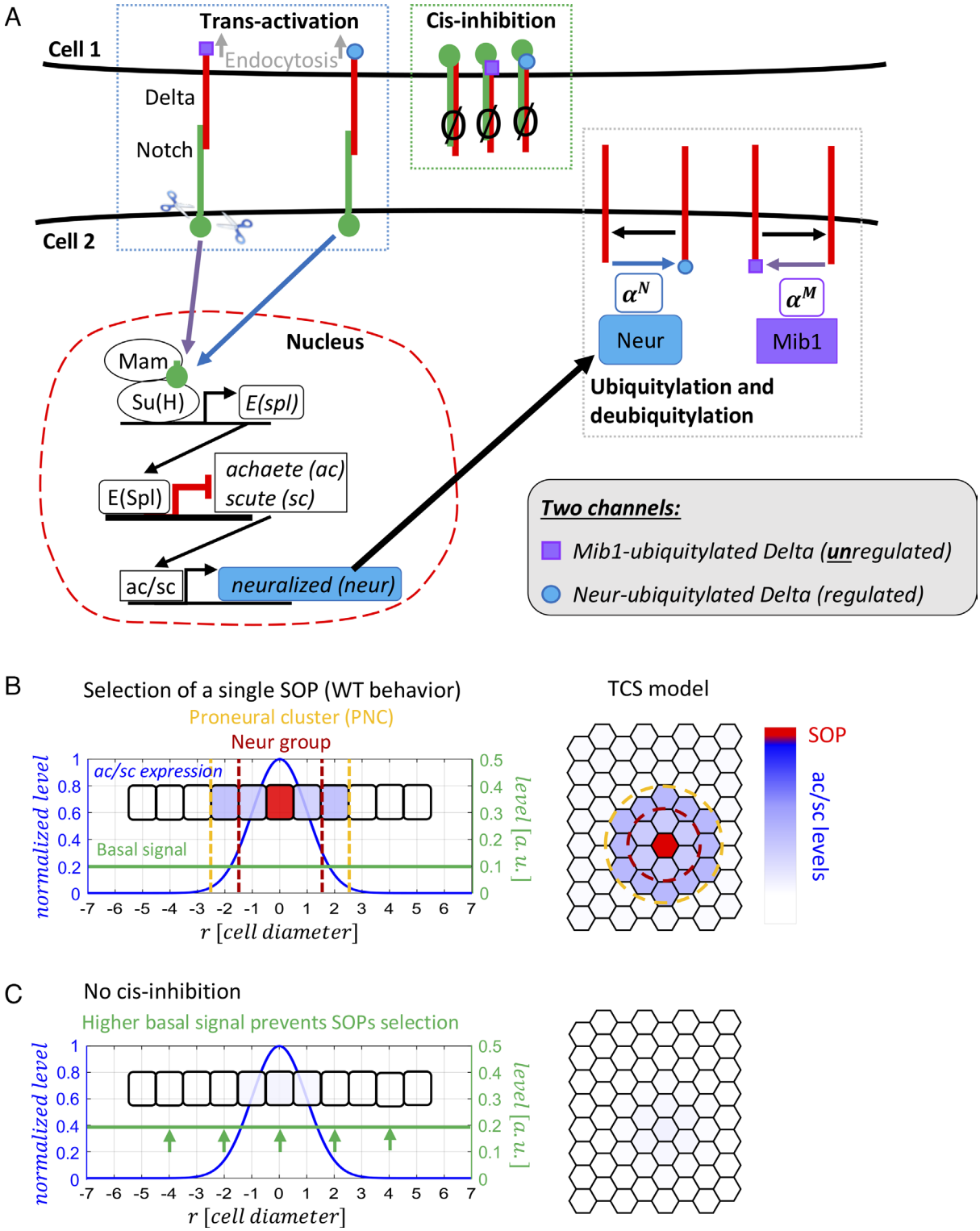

Fig. 1. The TCS model predicts the role of CI during SOP selection. (*A*) Schematics of the TCS model. Blue frame: Trans-activation of Notch receptors in cell 2 by Mib1- or Neur-ubiquitylated Dl in cell 1. Red frame: Transcriptional regulation of Ac/Sc and Neur by Notch activity. Gray frame: Ubiquitylation of Dl by Mib1 (not regulated by Notch activity) and Neur (regulated by Notch activity), with respective ubiquitylation rates α^M and α^N. Mib1- or Neur-ubiquitylated Dl can get deubiquitylated. Green frame: Cl between Dl and Notch in the same cell forms an inactive complex (Ø sign), which prevents trans-activation via the cis-inhibited ligand and receptor. (*B* and *C*) Selection of SOP depends on the strength of CI. (*B*) Simulation of the TCS model using the default parameters and the Ac/Sc-expression profile (blue curve) (*Materials and Methods*, *SI Appendix*, Table S1 and Fig. S1). Resulting Ac/Sc levels (color-bar) showing the selection of a single SOP (red cell). Cells in the Neur group (red dashed line/circle) are inhibited from becoming SOPs by Neur-mediated signaling (lateral inhibition) from the SOP. Cells inside the PNC (yellow dashed line/circle), and outside the Neur group, are inhibited from becoming SOPs by Mib1-mediated signaling (basal signal, green line) among all cells. Cells outside the PNC have a too-low Ac/Sc expression to become SOPs (and are also inhibited by the basal signal). (*C*) Loss of CI, by setting the CI rate to zero ($K_c = 0$, *SI Appendix*, Table S1), leads to the loss of SOP selection due to an increase in the basal Notch signal, mediated by Mib1. In this case, the basal signal is increased by 80%, relative to the WT condition in (*B*).

CI-Deficient Ligands in *Drosophila*. In order to experimentally validate the predictions of the TCS model regarding the role of CI in SOP selection, we used murine Dll1, which has been reported to possess only very weak or even no cis-inhibitory abilities (23). The cis-inhibitory abilities of ligands can be revealed by their expression in the wing primordium with *ptc*Gal4, which drives expression in a broad stripe of cells at the anterior side of the A/P compartment boundary of the wing disc in a gradient that increases toward the posterior (Fig. 2 *A*–*A*″). Dl expressed in this gradient induces the ectopic expression of the Notch target gene *wg* in two parallel stripes in the dorsal and ventral compartments of the wing (24) (Fig. 2 *B*–*B*″). The common understanding of the formation of these two stripes is that Dl suppresses Notch activity in regions of high expression due to CI but activates Notch in the adjacent posterior cells and also in anterior regions of low expression (Fig. 2*B*″). In agreement with the notion that CI depends on the ratio between Notch-receptors and ligands, coexpression of Dl with Notch suppressed CI and leads to ectopic expression of Wg throughout the *ptc*Gal4 gradient (Fig. 2*C*).

We found that the expression of Dll1 induced a broad band of ectopic Wg-expression, similar to coexpression of Dl with Notch (Fig. 2 *D* and *F*, compare with Fig. 2*C*). No region devoid of Wg expression was observed. This is a behavior very similar to the truncated SerΔEGF6, which has been shown to lack CI (*SI Appendix*, Fig. S2 *A*–*C*′) (25). To further test whether the cis-inhibitory abilities of Dll1 are indeed reduced, we coexpressed two Dll1 insertions to achieve even higher levels of Dll1 expression (4, 16). We found no evidence for CI upon coexpression of two copies of Dll1 (Fig. 2*E*). In contrast, expression of Dll1 with the cis-inhibitory Dl resulted in the suppression of Wg expression in the *ptc*Gal4 expression domain, indicating that CI is imposed by Dl, even in the presence of Dll1 (*SI Appendix*, Fig. S2*D*, arrow). Altogether, these results suggest that Dll1 has no or strongly reduced cis-inhibitory abilities at least at the functional level.

Expression of ligand variants in MARCM clones in the wing primordium of the wing imaginal disc confirmed the deficiency in CI of Dll1 (*SI Appendix*, Fig. S2 *E*–*G*′). While expression of Dl induces strong expression of Wg in cells adjacent to the clone, but much weaker or no expression within the clone (*SI Appendix*, Fig. S2 *E* and*E*′, arrow), Dll1 and the CI-lacking SerΔEGF6 induced strong levels of Wg- expression and also that of another target gene, Cut, throughout the clones, as well as in adjacent cells (*SI Appendix*, Fig. S2 *F*, *G*′, and *I*–*J*′, arrow). Note that NICD-expressing MARCM clones behave in a similar manner (*SI Appendix*, Fig. S2 *H* and *H*′, arrow).

Altogether, these results confirmed that Dll1 is a ligand that has only weak or no cis-inhibitory abilities in *Drosophila*. Since we cannot completely rule out the possibility that the behavior of

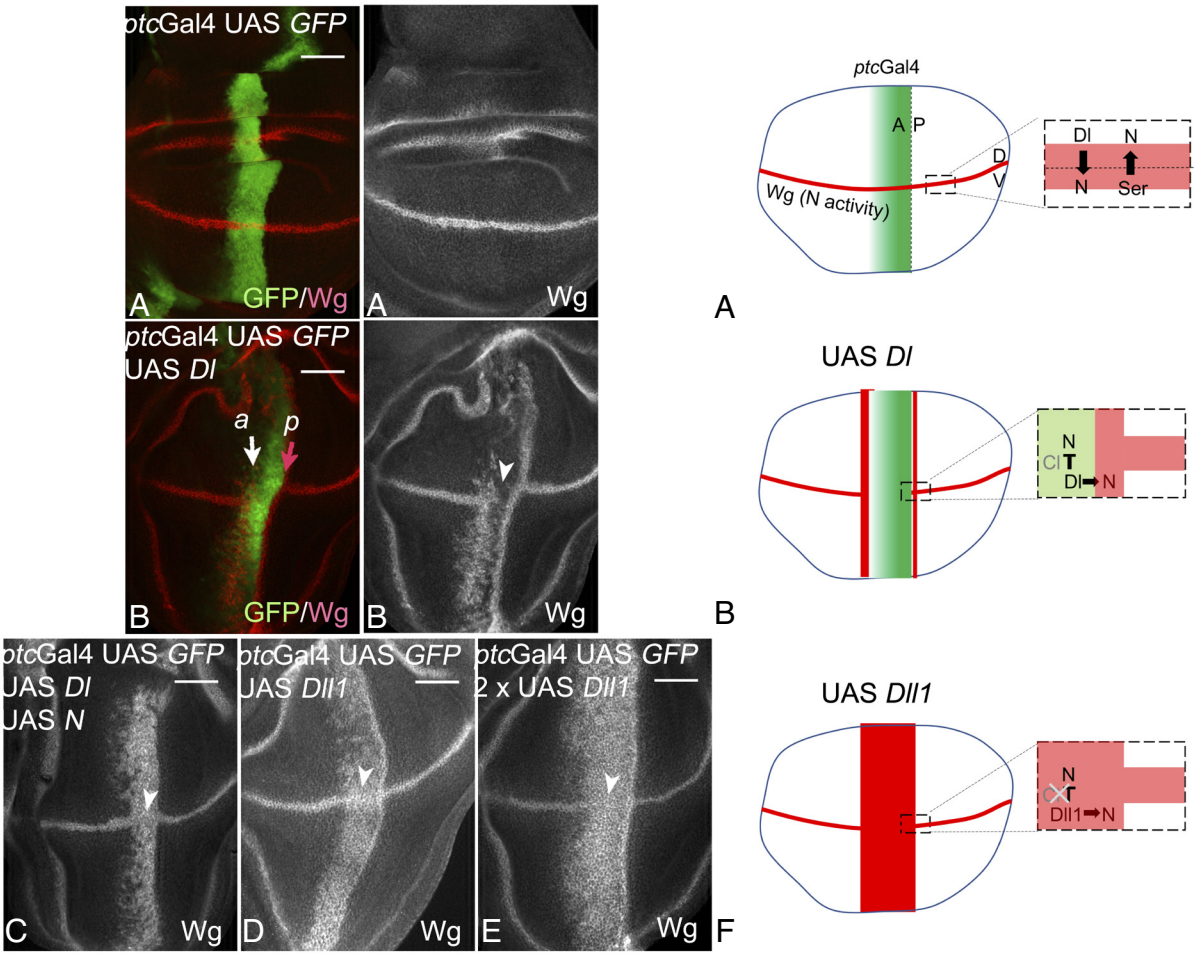

Fig. 2. Dll1 is Cl-deficient in Drosophila. (*A*–*A*″) *ptc*Gal4 drives expression of UAS constructs in a band along the anterior side of the A/P-boundary (see *A*″). The expression is graded, decreasing toward the anterior side. It intersects the stripe-like expression domain of Wg along the D/V-compartment boundary. (*B*–*B*″) Expression of Dl with *ptc*Gal4 results in the induction of two ectopic stripes of Wg expression perpendicular to its endogenous domain with no expression between them (arrowhead). The suppression of the endogenous expression of Wg is a hallmark of CI. (*C*) Coexpression of Notch (N) with Dl suppresses CI and results in the ectopic expression of Wg throughout the whole *ptc*Gal4 domain. No suppression of the endogenous Wg domain is observed (arrowhead). (*D*–*F*) Similarly, ectopic expression of one (*D*) or two (*E*) copies of Dll1 in the *ptc*Gal4 domain does not cause CI (arrowhead). (Scale bars for *A*–*E*: 50 μm.)

Dll1 is caused by strong trans-activation relative to its cis-inhibitory abilities, we use the term CI-deficient throughout this work, which indicates that it lacks CI at the functional level.

CI Is Required for SOP Selection in the Notum and Wing. To test the predictions of the TCS model regarding the requirement for CI (Fig. 1*C*), we employed the established assay where the Dl-variants are expressed uniformly in *Dl/Ser*-mutant cell clones with the MARCM system (10). As captured by the TCS model (Fig. 3 *A*–*B*‴), the concomitant loss of *Dl* and *Ser* in PNCs of the notum results in a strong neurogenic phenotype where all mutant cells of a PNC adopt the SOP fate, indicated by the expression of the SOP marker Hindsight (Hnt) and the formation of tufts of bristles in the corresponding imago (Fig. 3 *A*–*B*). Ubiquitous expression of Dl in the *Dl/Ser*-mutant cells by *tub*Gal4 (MARCM clones) reestablishes the selection process and the bristle pattern in the imago (10, 17)

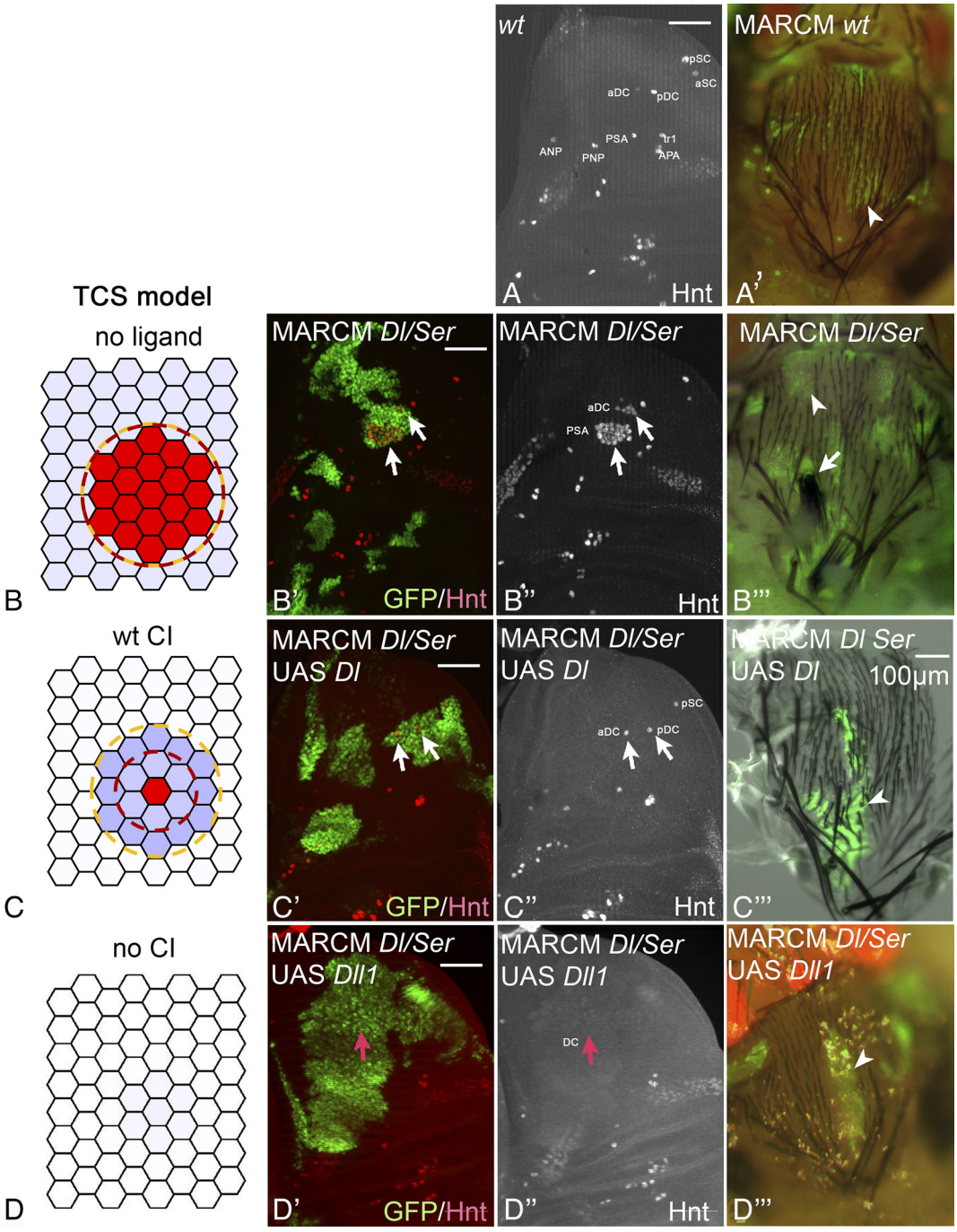

Fig. 3. CI is required for SOP selection in the notum. (*A* and *A*′) SOP pattern in a late third instar wing disc revealed by Hnt expression (*A*) and bristles of the adult WT notum (*A*′). GFP expression marks a WT MARCM clone (arrowhead). (*B*–*B*‴) The effect of *Dl/Ser*-MARCM clones on the SOP pattern. The TCS model (*B*) predicts a strong neurogenic phenotype in the absence of ligands. *Dl/Ser*-MARCM clones (arrows in *B*′) display a strong neurogenic phenotype within the clones in the wing disk (arrows) and the formation of tufts of bristles in the case of the large sensory bristles (arrow in *B*″) and loss of the external parts of small sensory bristles (arrowhead in *B*″). (*C*–*C*‴) The effect of *Dl/Ser*-MARCM clones expressing Dl on the SOP pattern. The TCS model (*C*) predicts a single SOP when a WT ligand (with CI) is uniformly expressed (same as Fig. 1*B*). Experiments with *Dl/Ser*-MARCM clones expressing Dl (arrows in *C*′) show a normal SOP phenotype within the clones in the wing disk (arrows in *C*″) and in an adult notum (arrowheads in *C*‴). (*D*–*D*‴) The effect of *Dl/Ser*-MARCM clones expressing Dll1 on the SOP pattern. The TCS model (*D*) predicts no SOP when a ligand with no CI is used (same as Fig. 1*C*). The *Dl/Ser*- MARCM clones expressing Dll1 (red arrow in *D*′) show no SOP forming within the clones (red arrow in *D*″) and no bristles in the adult notum (arrowhead in *D*‴). See *SI Appendix*, Table S1 for parameters used in simulations (*B*–*D*). (Scale bars for *A*–*D*: 50 µm, except *C*‴: 100 µm.)

(Fig. 3 *C*–*C*‴). We next monitored the consequences of expression of the CI-deficient Dll1 for SOP development in two different developmental contexts: in the notum and in the wing. If not mentioned otherwise, the MARCM clone cells are double mutant for *Ser* and *Dl*.

Analysis in the Notum. In contrast to *Dl*, the expression of Dll1 in MARCM clones completely suppressed the formation of SOPs (Fig. 3 *D*–*D*‴), confirming the prediction of the TCS model (Fig. 1*C*). No Hnt-positive cells emerged in the clonal areas. The clones of freshly hatched or late pupal flies were devoid of bristles confirming that bristle development is abolished. The observed phenotype of Dll1-MARCM clones resembled that of expression of the activated form of Notch (NICD) (*SI Appendix*, Fig. S3 *A* and *A*′).

To ensure that Dll1 activates Notch at least as much as Dl, we looked at the response of the Notch activity reporter Gbe+Su(H) in the MARCM clones (*SI Appendix*, Fig. S3 *B*–*D*′) (26). We observed a strong increase in the expression of Gbe+Su(H) in Dll1-expressing MARCM clones in comparison to Dl-expressing clones, indicating that Dll1-expression induces higher levels of Notch activity than Dl-expression (compare *SI Appendix*, Fig. S3 *C* and *C*′ to *SI Appendix*, Fig. S3 *D* and *D*′). This conclusion was corroborated by coexpressing a *Notch-RNAi* construct along with Dll1 in MARCM clones. In this case, we observed a strong neurogenic phenotype, indicating that activation by Dll1 requires Notch (*SI Appendix*, Fig. S3 *E* and *E*′). Consistent with these experimental results, a simulation of the TCS model where both CI and Notch-expression rates are set to zero results in the strong neurogenic phenotype (*SI Appendix*, Fig. S3*F*).

Finally, the expression of SerΔEGF6 in *Dl/Ser*-double mutant MARCM clones also leads to suppression of SOP formation phenocopying the behavior of Dll1 (*SI Appendix*, Fig. S3 *G* and *G*′). In summary, the presented results support the prediction of the TCS model that ligands that lack CI cannot mediate SOP selection in the notum.

A critical parameter for CI is the ligand/Notch ratio (4, 24). We therefore aimed to suppress CI of the endogenous ligands during SOP selection by elevating the levels of Notch. To do so, we overexpressed Notch in MARCM clones. Overexpression of Notch in WT cells led to an increase in activation of the Notch pathway, indicated by elevated expression of the Gbe+Su(H) Notch-activity reporter (*SI Appendix*, Fig. S4 *A* and *A*′). It also suppressed SOP formation and bristle development (*SI Appendix*, Fig. S4 *B*–*B*″). This suppression required the presence of the endogenous ligands since it was abolished in *Dl/Ser*-mutant MARCM clones expressing Notch (*SI Appendix*, Fig. S4 *C* and *C*′). Thus, suppression of CI by the endogenous ligands by increasing receptor/ligand ratio also results in a failure of SOP formation.

Analysis in the Wing. The SOPs of the bristles of the anterior wing margin are determined during the late third instar stage in two stripes along the anterior half of the D/V-boundary, adjacent to the domain of Wg expression (Fig. 4 *A*–*A*″). Notch signaling induces the expression of the secreted Wg along the D/V boundary, which in turn induces the two stripe-like PNCs adjacent to it [(3, 27); Fig. 4*A*″]. In the established PNCs, Dl signaling is required for the selection of the SOP. Thus, the Notch-pathway is indirectly (via induction of Wg expression) required to establish the PNC and subsequently to select the SOP within it. Ectopic SOP development can be induced in the wing blade by expression of Wg or Dl (27) (Fig. 4 *B*–*C*″). In the case of ectopic Wg expression, the arising SOPs are regularly distributed and well separated from each other (Fig. 4 *B*–*B*″). Note that this pattern of SOPs is predicted by the TCS model with uniformly high Ac/Sc levels (*SI Appendix*, Fig. S1*A*′). As expected, knocking down Notch in Wg-expressing MARCM clones resulted in a strong neurogenic phenotype (*SI Appendix*, Fig. S5 *A*–*A*″). MARCM clones that expressed Dl induced two PNCs, one less defined inside the clone and one well-defined stripe-like PNC outside the clone (Fig. 4*C*, C', arrow). The PNCs give rise to well-separated SOPs that express Hnt (Fig. 4 *C*–*C*″).

The expression of Dll1 resulted in a failure of SOP formation inside the clone but did not affect SOP development outside (Fig. 4 *D*–*D*″, arrow). The suppression of SOP development inside the Dll1-expressing clone was relieved upon depletion of Notch (*SI Appendix*, Fig. S5 *B*–*B*″). A similar phenotype was induced by

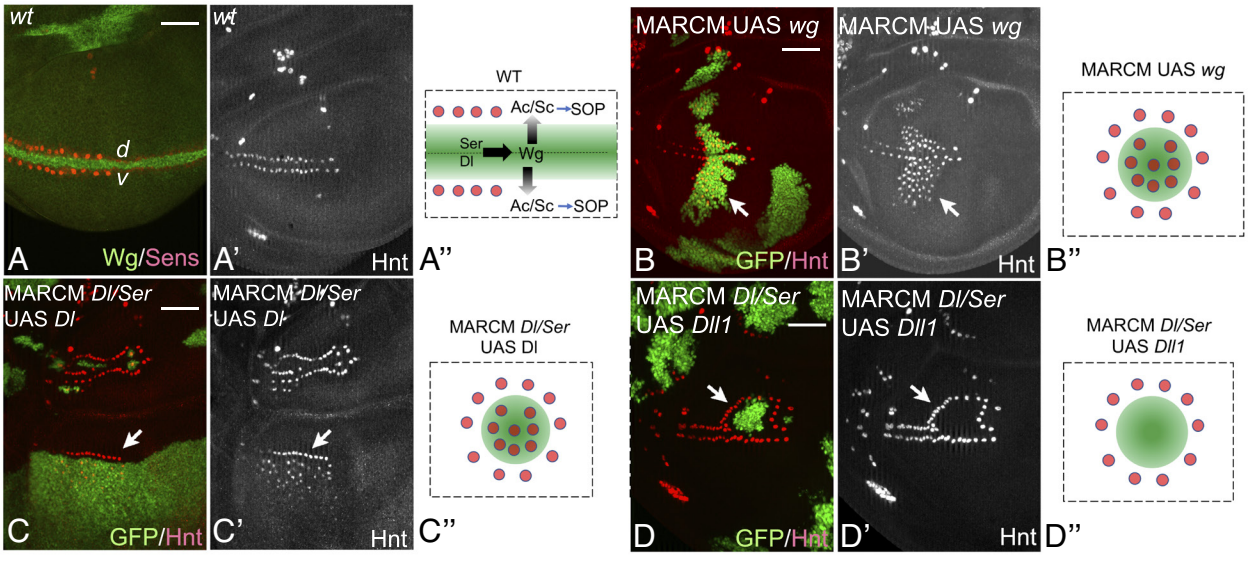

Fig. 4. CI is required for the selection of the SOP in the wing. (*A*–*A*″) Induction of SOP formation along the D/V compartment boundary in the anterior compartment by Notch and Wg. The activity of the Notch pathway induced by mutual signaling of Ser and Dl establishes the expression of Wg along the D/V boundary. Wg secreted by the boundary cells induces the expression of Ac/Sc in adjacent dorsal and ventral cells to establish two stripe-like PNCs from which the SOPs are selected via Notch signaling. (*B*–*B*″) Ectopic expression of Wg via MARCM clones results in the establishment of ectopic PNCs and ectopic SOPs within the clone (inside PNC) and outside the clone (outside PNC, arrow). The SOPs are well separated because of the Notch-mediated lateral inhibition process (Fig. 4 and *SI Appendix*, Fig. S1 *A* and *A*″). (*C*–*C*″) Expression of Dl in *Dl/Ser*-MARCM clones induces SOP formation inside and outside the clone (arrow). (*D*–*D*″) In contrast to Dl, the expression of Dll1 in *Dl/Ser*-MARCM clones suppresses SOP formation in the clone but induces it outside the clone. (Scale bar: 50 μm.)

coexpression of Dl with Notch to suppress CI in MARCM clones (*SI Appendix*, Fig. S5 *C–C″*), or expression of SerΔEGF6 (Fig. 6 *C* and *C′*). These findings confirm that CI is necessary to allow SOP formation to occur, also in the ectopically induced PNCs.

Ligands Deficient for CI Prevent the Formation of the Neur Group. We next tested whether CI is required for the formation of the Neur group. To do so, we asked whether Neur-expressing cells are observed in the presence or absence of CI in a MARCM clone setup. We observed Neur-expressing cells in MARCM clones that express Dl, but not in clones that express Dll1, suggesting that a Neur group has formed only in the Dl-expressing clones (*SI Appendix*, Fig. S5 *D–E″* and Fig. 5 *A–B′*).

It has been previously shown that *neur* mutants display a weak neurogenic phenotype because only the Neur group adopts the SOP fate (12, 28, 29) (*SI Appendix*, Fig. S6). This observation is captured in the TCS model with the same set of parameters if the expression rate of Neur is set to zero (Fig. 5*C*). The subset of cells adopting the SOP fate is expected to be those that express high enough levels of Ac/Sc to overcome the basal Notch activity provided by the nonregulated channel. Indeed, MARCM clones that lack the *neur* function and express Dl showed the weak neurogenic phenotype in both the wing and the notum (Fig. 5 *C′–C‴″*). We next asked whether removing CI will suppress Neur expression in these cells. The TCS model predicted that in the absence of both Neur expression and CI (i.e., setting both the Neur expression and CI rates to zero in the model), the basal Notch activity would significantly increase, resulting in a decrease of Ac/Sc levels and in suppression of the weak neurogenic phenotype (Fig. 5*D*). This prediction was validated experimentally as *neur*-mutant MARCM clones that express Dll1 showed no SOP development (Fig. 5 *D′–D‴″*). This shows that, in contrast to ligands with cis-inhibitory abilities, ligands deficient for CI suppress SOP development in a Neur-independent manner. Combined with the finding that expression of Dll1 prevents the expression of Neur, these results support the notion that the enhanced basal Notch activity with the CI-deficient ligands above the threshold prevents the definition of the Neur group and therefore prevents the selection of the SOP.

Enhanced CI Results in an Excess of SOPs. We next wanted to test the effect of enhanced CI on SOP selection. The TCS model predicts that increasing CI, without changing any other parameter, should result in a corresponding increase in the number and density of SOPs (Fig. 6*A*). This is because CI suppresses the basal Notch activity, which expands the domain of the Neur group within the PNC. The model further predicts that strong-enough CI (relative to the trans-activation channels) in the PNC renders the cells more

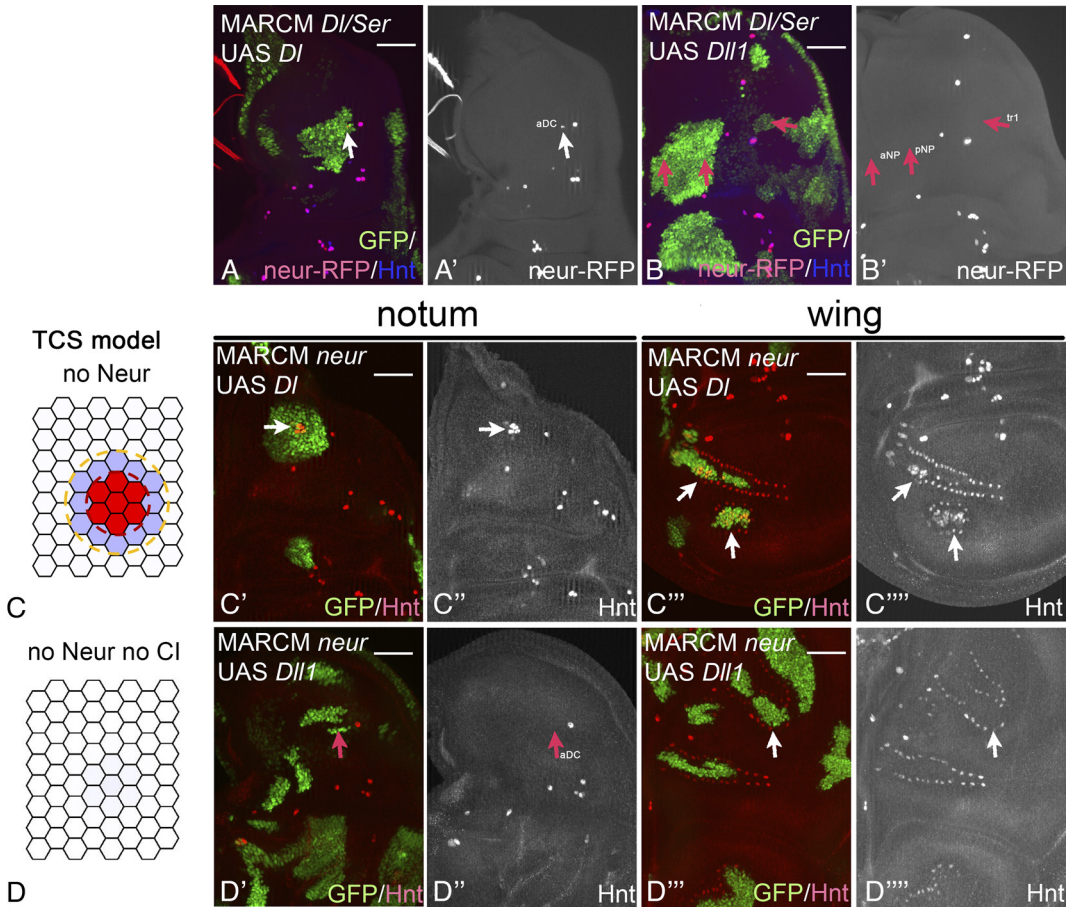

Fig. 5. The formation of the Neur group requires CI. (*A–B′*) Expression of Neur in the future SOP is observed only in *Dl/Ser*-MARCM clones that express a cis-inhibitory ligand. (*A* and *A′*) *Dl/Ser*-MARCM clone expressing Dl shows a single Neur-expressing SOP within the clone (arrow). (*B* and *B′*) Expression of Dll1 in clones suppresses SOP formation in the clone (arrows) and Neur expression is absent in the clone cells. (*C–C‴″*) The effect of *neur*-MARCM clones (no Neur within the clone) expressing Dl on the SOP pattern. The TCM model (*C*) predicts that in the absence of Neur, a subgroup of cells within the PNC (the Neur group) will emerge when a WT ligand (with CI) is uniformly expressed. *neur*-MARCM clones expressing Dl in the notum (arrows in *C′* and *C″*) and in the wing disk (arrows in *C‴* and *C‴″*) show the formation of small groups of SOPs within the clones (weak neurogenic phenotype). (*D–D‴″*) The effect of *neur*-MARCM clones (No Neur within the clone) expressing Dll1 on the SOP pattern. The TCM model (*D*) predicts that in the absence of Neur and with no CI, no SOPs will be formed. *neur*-MARCM clones expressing Dll1 in the notum (arrows in *D′* and *D″*) and in the wing disk (arrows in *D‴* and *D‴″*) show no SOPs within the clones. The result suggests that CI is required for the formation of the Neur group. See *SI Appendix*, Table S1 for parameters used in simulations (*C*), and (*D*). (Scale bar: 50 μm.)

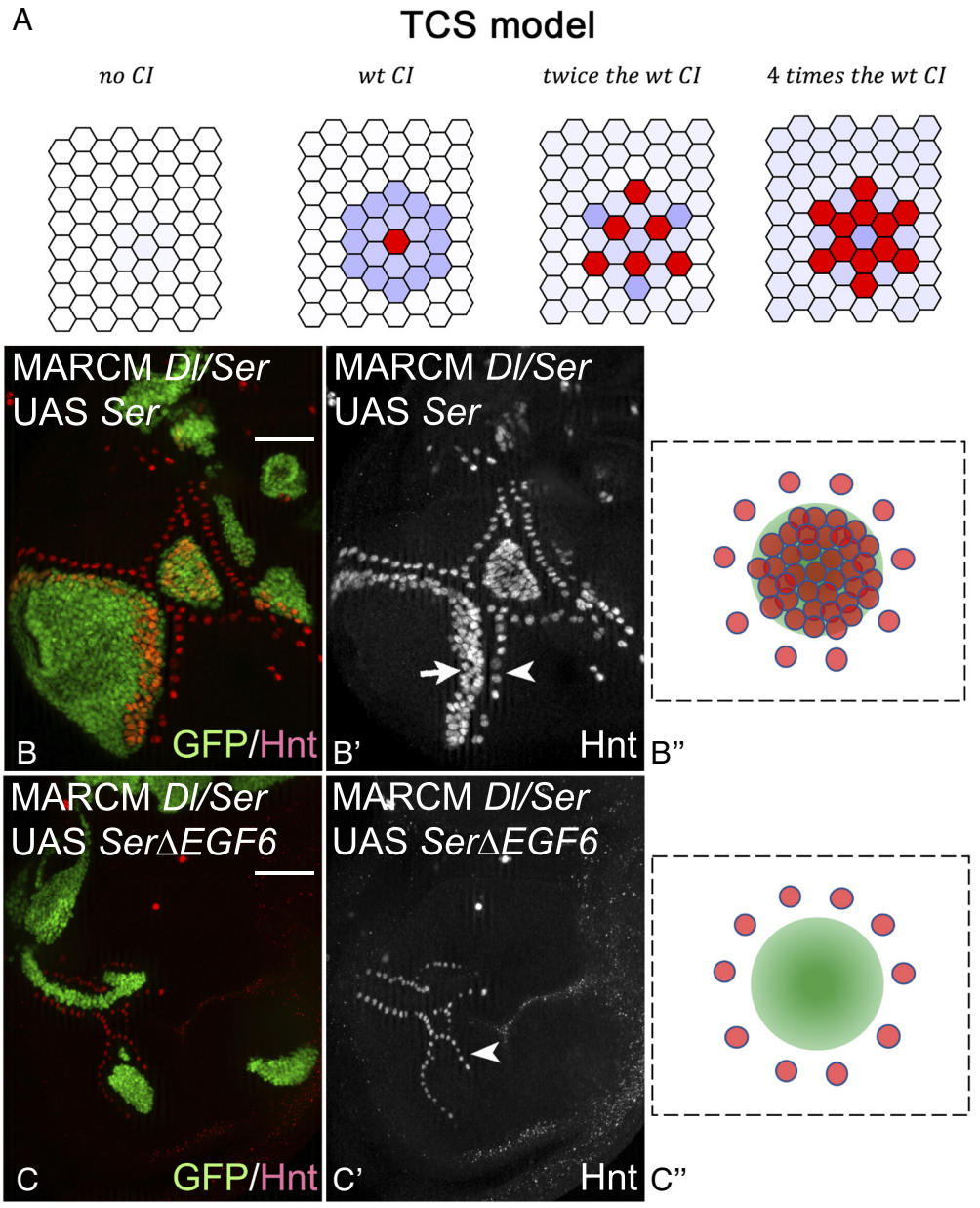

Fig. 6. Ligands with strong CI promote formation of extra SOP. (*A*) The TCS model shows that an increase in the strength of CI leads to the formation of extra SOPs. The relative level of CI strength (*Materials and Methods* and *SI Appendix*, Table S1) compared to the WT parameter are as indicated. (*B*–*B*″) Expression of Ser in *Dl/Ser*-MARCM clones in the wing disc induces extra SOPs inside the clone (neurogenic phenotype, arrow) and normal SOPs outside the clone (arrowhead). (*C*–*C*″) In contrast, the expression SerΔEGF6 suppresses SOP formation inside the clone completely. The SOPs outside the clone are still generated (arrowhead), indicating that SerΔEGF6 can signal in trans. (Scale bar: 50 μm.)

refractory to trans-activation. As a result, a denser SOPs pattern with directly adjacent SOPs develops (See Fig. 6*A* "4 times wt CI"). It has been shown that Ser is more cis-inhibitory than Dl in the wing primordium (4, 30). We therefore monitored the effect of high CI of Ser on the selection of the SOP in the wing primordium. In agreement with the TCS model, the ectopic expression of Ser in *Dl/Ser* MARCM clones induced an excess of SOPs inside the clone (Fig. 6 *B*–*B*″, arrow), matching the model's prediction for stronger CI. However, like Dl, Ser also induced the formation of well-separated SOPs outside the clone (Fig. 6*B*′, arrowhead). In contrast, expression of the CI-lacking SerΔEGF6 suppressed SOP formation inside (but not outside) the clone (Fig. 6 *C*–*C*″, arrowhead). These results show that while reducing CI leads to loss of SOPs, increasing CI drives the formation of supernumerary SOPs.

A Compensation Mechanism between CI and the Unregulated Notch Channel. The overall picture that emerges from our analysis is that a key aspect in SOP selection is the interplay between basal Notch signaling (mediated by the unregulated channel) and CI, which suppresses the basal Notch signaling to a level that allows the formation of the Neur group. To test the role of the unregulated channel, we have simulated in the TCS model the cases where Mib1 is overexpressed (higher unregulated channel strength, Fig. 7*A*) and where Mib1 is removed (lower unregulated channel strength, Fig. 7*B*). The TCS model predicted that higher level of Mib1 should increase Notch activity and suppress SOP formation (Fig. 7*A*), while lower levels should lead to a decrease of Notch activity and the formation of extra SOPs (Fig. 7*B*). These predictions were matched by the corresponding experimental

observations (Fig. 7 *A′*–*B″*). We note that we have previously shown that Notch signaling still persists (albeit, at a lower level) even if *mib1* is knocked out (17). We therefore assumed in the simulation that the unregulated Notch channel strength is reduced but is not abolished in *mib1* mutants (*Materials and Methods*).

Next, we wanted to analyze the interplay between CI and the unregulated Notch channel. The TCS model predicts that formation of ectopic SOPs in *mib1* knockout, which leads to lower basal Notch signaling, can be rescued by the presence of a non-cis-inhibitory ligand, which promotes higher basal Notch signaling (Fig. 7*C*). This situation was simulated by setting both the CI rate to zero and reducing the unregulated channel strength by half. The TCS model in this case predicts the formation of a single SOP. We experimentally tested this prediction by looking at *Dl/Ser*-MARCM clones in an *mib1*-mutant wing discs that express Dll1. As predicted by the TCS model, single SOPs appeared within the clones, confirming the compensation mechanism between *mib1* activity and CI (Fig. 7 *C′*–*C‴*).

To better understand the interplay between the unregulated Notch channel and CI, we performed a comprehensive phase space analysis of the TCS model on the dependence of the SOP phenotype on the two key parameters of the system: the relative strength of CI and the relative strength of the signal from the unregulated channel (Fig. 7*D*). The phase space analysis provides a comprehensive view of how the phenotype (i.e., number of SOPs) depends on the strength of CI and the strength of the unregulated channel. Decreasing or increasing the strength of CI (moving horizontally in the Fig. 7*D*) would lead to a decrease or increase in the number of SOPs, respectively (corresponding to Figs. 3 *C–D‴* and 6). Similarly, increasing or decreasing the strength of the unregulated channel (moving vertically on the Fig. 7*D*, points A and B) would lead to a decrease or increase in the number of SOP, respectively (corresponding to Fig. 7 *A*–*B″*). Finally, decreasing both CI and the unregulated channel would lead to the WT SOP phenotype (point C in Fig. 7*D*, experimentally observed in Fig. 7 *C′*–*C‴*). Thus, the phase space analysis highlights the conclusion that a selection of a single SOP relies

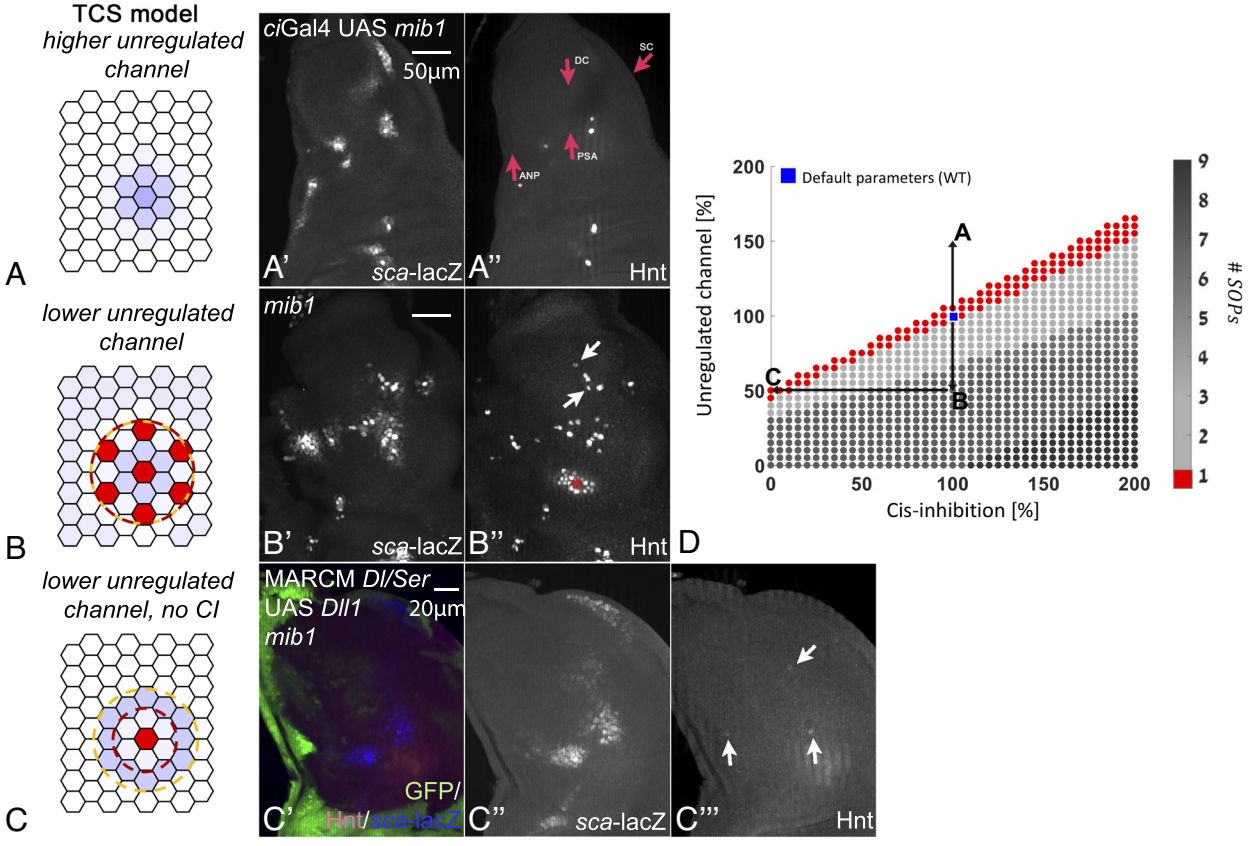

Fig. 7. A trade-off between CI and the unregulated Notch channel. (*A–A″*) The effect of Mib1 overexpression on SOP development. The TCS model (*A*) predicts that an increase of 50% in the activity of the unregulated channel, corresponding to higher Mib1 expression, should lead to suppression of SOP. Experiments where Mib1 was overexpressed showed that while PNCs are still defined (marked by *sca*-LacZ in *A′*), some of the SOPs within these PNCs are suppressed as predicted by the model (arrows in *A″*). (*B–B″*) The loss of *mib1* function results in the development of supernumerary SOPs. The TCS model (*B*) predicts that a reduction of 50% in the activity of the unregulated channel, corresponding to a reduced (but not completely suppressed) activity due to Mib1 knockout, should lead to the selection of more than one SOP from the PNC. Experiments where *mib1* function was deleted showed that PNCs are still defined (marked by *sca*-LacZ in *B′*), yet extra SOPs emerge within the clones, as predicted by the model (arrows in *A″*). (*C–C‴*). Loss of *mib1* function can be compensated by loss of CI. The TCS model (*C*) predicts that a reduction of 50% in the activity of the unregulated channel (as in *B*) together with suppression of CI should regain the WT phenotype of a single SOP. This prediction was realized experimentally by looking at *Dl/Ser*-MARCM clones expressing Dll1 (the region that lacks GFP in *C′*) in the background of a *mib1* knockout. As predicted experimentally, PNC within the clone (marked by *sca*-LacZ in *C″*) showed the emergence of a single SOP within each clone (arrows in *C‴*). (*D*) A phase diagram showing the TCS model predictions for a range of parameters. The *X* axis values refer to the relative levels of CI strength with respect to the WT CI value. The *Y* axis values refer to the relative levels of the unregulated channel strength, with respect to the value used to simulate the WT (*Materials and Methods*). The number of SOPs for each parameter set is shown by the color bar. The value used for simulating the WT (Blue square) and the mutant cases shown in (*A–C*) are indicated. See *SI Appendix*, Table S1 for parameters used in simulations (*A–D*). (Scale bar: 50 μm, except *C*: 20 μm.)

on the trade-off between Notch signaling from the unregulated channel and CI.

Discussion

The selection of the SOP is a classical, extensively studied, process mediated by Notch signaling where a single cell is selected from an equivalence group, the PNC. This process has been considered a prime example of selection by lateral inhibition. Here, we propose a model, the TCS model, for the selection of a single SOP from the PNC, which significantly differs from the classical models of lateral inhibition (referred to as the TFB models). The major aspects of the TCS model include the following: i) The Notch-ligand activity, rather than the ligand expression level, is regulated by Notch signaling. ii) Dl activity is regulated by two channels associated with the E3 ubiquitin ligases Neur and Mib1. While the *neur* channel is regulated by Notch activity, the *mib1* is not regulated by Notch activity and produces a broad basal Notch activity. iii) The PNC is defined by gradients of expression of Ac/Sc. Within the PNC, the subgroup that participates in the *neur*-controlled lateral inhibition process (the Neur group) is defined by both the gradient profile and the basal Notch activity driven by *mib1*. iv) CI is required for the suppression of basal Notch activity and determines the extent of the Neur group within the PNC.

The use of mammalian Dll1 and SerΔEGF6, which are deficient in CI, allowed us to show that CI is required for SOP selection and to test critical predictions of the TCS model. The TCS model can account for two earlier observations that could not be explained by the TFB model: i) that unregulated homogenous expression of Dl can also mediate SOP selection (10, 31) and ii) that loss of *ac* and *sc* did not affect Dl expression (11, 12).

The TCS model also accounts for the distinct mutant phenotypes of *Dl/Ser* (neurogenic phenotype), *neur* (weak neurogenic phenotype), and *mib1*. While in *Dl/Ser* clones, all the cells in the PNC become SOP, since signaling from both channels (*neur* and *mib1*) is removed, in the *neur* mutant, only the cells in the Neur group become SOPs, since basal Notch activity through Mib1 remains, and define the boundaries of the Neur group. The *mib1* mutant leads to extension of the Neur group and consequently leads to the formation of supernumerary, but well separated, SOPs. This is because Neur-mediated Notch activity still exists and lateral inhibition is not restricted anymore to a small subgroup. We note that a previous model suggested an explanation for the *neur* phenotype based on weaker nonlinear dependence of Dl activity on the proneural state (i.e., on Ac/Sc) (32). In contrast, in the TCS model, deletion of *neur* leads to complete independence of Dl activity on Ac/Sc; thus, it explains better the extent of the group of SOPs formed in the absence of lateral inhibition feedback.

Thus, the TCS model can explain the previously unexplained observations and captures the different Notch pathway phenotypes. It does so with a single set of parameters highlighting the robust nature of the proposed model. In contrast to previous models, our model relies only on Notch signaling between direct neighbors and does not invoke long-range signaling (32, 33). The selection of only one SOP is achieved by restricting the potential to be selected for an SOP to a smaller subgroup of the PNC through Mib1-mediated basal Notch activity. This does not rule out a contribution of longer-range signaling in other processes, for example, by filopodia-mediated Notch signaling (34, 35).

What is the role of CI in SOP selection? The overall picture that emerges from the TCS model and the experiments is that there is a trade-off between *mib1*-mediated basal Notch activity and the strength of CI. Without CI (replacing Dl by Dll1, or SerΔEGF6), there is a higher level of basal Notch activity, which completely abolishes the formation of SOP. With stronger CI, (replacing Dl by Ser) basal Notch activity is reduced and extra SOP emerges. Finally, by removing both CI (which increases basal activity) and *mib1* (which decreases basal activity), we get almost full compensation and regain a single SOP. Thus, CI is crucial for adjusting the level of basal Notch activity to determine the extent of the Neur group and for the selection of a single SOP.

We would like to point out that CI could still directly contribute to the lateral inhibition process by making sender cells more refractory to signals from their neighbors (as has been suggested by ref. 16). The TCS model further suggests that for strong-enough CI, this refractory behavior would lead to a denser SOP pattern (Fig. 6*A*). Consistent with this expectation, replacing Dl with the strong cis-inhibitory Ser ligand exhibits a denser SOP pattern (Fig. 6*B*).

Materials and Methods

Drosophila Methods.

Fly strains. UAS *Ser-HA*, UAS *Dl-HA*, UAS *Dl-NEQN2A-HA* (17), UAS *Dll1-HA* (36), UAS *NICD* (31), UAS *SerΔEGF6* (25), UAS N-LV (37), UAS *N-RNAi* (Bloomington stock centre: BDSC_7078), UAS wg^{E1} (38), UAS *mib1* (39), Dl^{rev10} e Ser^{RX82} FRT82B (40), $neur^{1}$ e FRT82B (41), $mib1^{EY09870}$ (39), Gbe+Su(H)-lacZ (26), *sca*-lacZ (Bloomington stock centre, BSC5403), *neur*-RFP (42), *ptc*GAL4 (43), and *ci*GAL4 (44)

Stocks for MARCM analysis.

yw *hs*Flp *tub*GAL4 UAS GFPnls; FRT82B *tub*GAL80/TM2,
yw *Ubx*Flp *tub*GAL4 UAS GFPnls; FRT82B *tub*GAL80 y+/TM6 (Bloomington Stock Centre)
yw *Ubx*Flp; *ci*GAL4/CyOTb1; $mib1^{EY09870}$ FRT82B *ubi*GFP *tub*GAL80/TM6B

Clonal Analysis.

Clones were induced at the first larval instar stage (24 to 48 h after egg laying) by heat shock (*hs*Flp, 1 h at 37 °C) or by *Ubx*Flp.

Genotypes of the flies of the experiments.

Fig. 2:
(Fig. 2 *A* and *A′*) *w; ptcGAL4 UASGFP/+*;
(Fig. 2 *B* and *B′*) *w; ptcGAL4 UASGFP/UASDl-HA (51C)*;
(Fig. 2*C*)*w; ptcGAL4 UASGFP/UASDl-HA(51C), UASN-LV*;
(Fig. 2*D*) *w; ptcGAL4 UASGFP/UASDll1-HA (51C)*;
(Fig. 2*E*) w; ptcGAL4UASGFP/UASDll1-HA (51C);+/UASDll1-HA.

Fig. 3:

(Fig. 3 *A* and *A′*) *yw hsFlp tubGAL4 UASGFPnls; +/+;tubGAL80 FRT82B/FRT82B*;
(Fig. 3 *B′–B‴*) *yw hsFlp tubGAL4 UASGFPnls; +/+ ;tubGAL80 FRT82B/*Dl^{rev10} e^{1} Ser^{RX82} *FRT82B*;
(Fig. 3 *C′–C‴*) *yw hsFlp tubGAL4 UASGFPnls; +/UASDl-HA 51C; tubGAL80 FRT82B/*Dl^{rev10} e^{1} Ser^{RX82} *FRT82B*;
(Fig. 3 *D′–D‴*) *yw hsFlp tubGAL4 UASGFPnls; +/UASDll1-HA 51C; tubGAL80 FRT82B/*Dl^{rev10} e^{1} Ser^{RX82} *FRT82B*.

Fig. 4:

(Fig. 4 *A* and *A′*) *yw hsFlp tubGAL4 UASGFPnls; +/+; tubGAL80 FRT82B/FRT82B*;
(Fig. 4 *B* and *B′*) *yw hsFlp tubGAL4 UASGFPnls; +/UAS wg; tubGAL80 FRT82B/*Dl^{rev10} e^{1} Ser^{RX82} *FRT82B;*
(Fig. 4 *B* and *B′*) *yw hsFlp tubGAL4 UASGFPnls; +/UAS wg; tubGAL80 FRT82B/FRT82B*;
(Fig. 4 *C–C″*) *yw hsFlp tubGAL4 UASGFPnls; +/UASDl-HA 51C; tubGAL80 FRT82B/*Dl^{rev10} e^{1} Ser^{RX82} *FRT82B;*
(Fig. 4 *D–D″*) *yw hsFlp tubGAL4 UASGFPnls; +/UASDll1-HA 51C; tubGAL80 FRT82B/*Dl^{rev10} e^{1} Ser^{RX82} *FRT82B*.

Fig. 5:

(Fig. 5 *A* and *A′*) *yw hsFlp tubGAL4 UASGFPnls*; *+/UASDl-HA 51C, neur.H2B-mRFP; tubGAL80 FRT82B/*Dl^{rev10} e^{1} Ser^{RX82} *FRT82B;*

(Fig. 5 *B–B″′*) *yw hsFlp tubGAL4 UASGFPnls; +/UASDll1-HA 51C, neur.H2B-mRFP; tubGAL80 FRT82B/Dl^{rev10} e^{1} Ser^{RX82} FRT82B;*
(Fig. 5 *C–C″′*) *yw hsFlp tubGAL4 UASGFPnls; +/UASDl-HA 51C; tubGAL80 FRT82B/neur^{IF65} FRT82B;*
(Fig. 5 *D–D″′*) *yw hsFlp tubGAL4 UASGFPnls; +/UASDll1-HA 51C; tubGAL80 FRT82B/neur^{IF65} FRT82B.*

Fig. 6:

(Fig. 6 *B* and *B′*) *yw hsFlp tubGAL4 UASGFPnls; +/UAS-Ser 51C; tubGAL80 FRT82B/Dl^{rev10} e^{1} Ser^{RX82} FRT82B;*
(Fig. 6 *C* and *C′*) *yw hsFlp tubGAL4 UASGFPnls; +/UAS-SerDEGF6; tubGAL80 FRT82B/Dlrev10 e^{1} SerRX82 FRT82B.*

Fig. 7:

(*A*) *UASmib1/w; +/sca-lacZ; +/CiGAL4;*
(*B*) *w; sca-lacZ/+; mib1^{EY09780}/mib1^{EY09780};*
(*C*) *yw ubxFlp/; CiGAL4/UASDll1-HA 51C; mib1^{EY09780} FRT82B ubi.GFP tub.GAL80/mib1^{EY09780} FRT82B Dl^{rev10} e^{1} Ser^{RX82}.*

SI Appendix, Fig. S2:

(*A*) *w; ptcGAL4 UASGFP/UASSer HA(51C);*
(*B*) *w; ptcGAL4 UASGFP/UASSer-HA (51C), UASN-LV;*
(*C*) *w; ptcGAL4 UASGFP/UAS-SerDEGF6;*
(*D*) *yw hsFlp tubGAL4 UASGFPnls; +/UAS Dl-HA 51C; tubGAL80 FRT82B/FRT82B;*
(*E*) *yw hsFlp tubGAL4 UASGFPnls; +/UAS Dll1-HA 51C; tubGAL80 FRT82B/FRT82B;*
(*F*) *yw hsFlp tubGAL4 UASGFPnls; +/UAS UAS NICD; tubGAL80 FRT82B/FRT82B.*

SI Appendix, Fig. S3:

(*A*) *yw hsFlp tubGAL4 UASGFPnls; +/UAS NICD; tubGAL80 FRT82B/FRT82B;*
(*B*) *Gbe+Su(H)-lacZ;*
(*C*) *yw hsFlp tubGAL4 UASGFPnls/Gbe+Su(H)-lacZ; +/UASDl-HA 51C;tubGAL80 FRT82B/Dl^{rev10} e^{1} Ser^{RX82} FRT82B;*
(*D*) *yw hsFlp tubGAL4 UASGFPnls/Gbe+Su(H)-lacZ; +/UASDll1-HA 51C; tubGAL80 FRT82B/Dl^{rev10} e^{1} Ser^{RX82} FRT82B ;*
(*E*) *yw hsFlp tubGAL4 UASGFPnls/UASN-RNAi; +/UASDll1-HA 51C; tubGAL80 FRT82B/Dl^{rev10} e^{1} Ser^{RX82} FRT82B ;*
(*G*) *yw hsFlp tubGAL4 UASGFPnls; +/UAS-SerDEGF6; tubGAL80 FRT82B/Dl^{rev10} e^{1} Ser^{RX82} FRT82B.*

SI Appendix, Fig. S4:

(*A* and *B*) *yw hsFlp tubGAL4 UASGFPnls; +/UAS N-LV; tubGAL80 FRT82B/FRT82B;*
(*C*) yw hsFlp tubGAL4 UASGFPnls; +/UAS N-LV ; tubGAL80 FRT82B/*Dl^{rev10} e^{1} Ser^{RX82} FRT82B.*

SI Appendix, Fig. S5:

(*A*) *yw hsFlp tubGAL4 UASGFPnls/UASN-RNAi ; +/UASwg; tubGAL80 FRT82B/Dl^{rev10} e^{1} Ser^{RX82} FRT82B;*
(*B*) *yw hsFlp tubGAL4 UASGFPnls/UASN-RNAi; +/UASDll1-HA 51C; tubGAL80 FRT82B/Dl^{rev10} e^{1} Ser^{RX82} FRT82B ;*
(*C*) *yw hsFlp tubGAL4 UASGFPnls; +/UASDl-HA 51C, UASN-LV; tubGAL80 FRT82B/Dl^{rev10} e^{1} Ser^{RX82} FRT82B ;*
(*D*) *yw hsFlp tubGAL4 UASGFPnls; +/UASDl-HA 51C, neur.H2B-mRFP ; tubGAL80 FRT82B/Dl^{rev10} e^{1} Ser^{RX82} FRT82B ;*
(*E*) *yw hsFlp tubGAL4 UASGFPnls; +/UASDll1-HA 51C, neur.H2B-mRFP; tubGAL80 FRT82B/Dl^{rev10} e^{1} Ser^{RX82} FRT82B.*

SI Appendix, Fig. S6:

(*A*) *w; ptcGAL4 UASFlp/+; FRT82B ubi.GFP/FRT82B neur^{IF65}.*

Antibody Staining and Imaging. Antibody staining was performed according to standard protocols (Klein, 2006). Antibodies used were anti-Wg (4D4) (DSHB Iowa RRID:AB_528512), anti-ß-Gal (Cappel/MP Biomedicals RRID:AB_2313831), anti-Senseless (Nolo et al. 2000), anti-Hnt (1G9) (DSHB RRID:AB_528278), anti-ELAV (7E8A10) *(DSHB* RRID:AB_528218), and anti-futsch (22C10) (DSHB RRID:AB_528403). Alexa-Fluorochrome-conjugated secondary antibodies were purchased from Invitrogen/Molecular Probes. Images were acquired with a Zeiss AxioImager Z1 Microscope equipped with a Zeiss Apotome/Apotome2.

Model. For the full derivation of the TCS model, please see *SI Appendix*. This derivation includes a detailed description of the reactions in Fig. 1*A*, formalization of these reactions in a set of differential equations, a steady-state analysis and assumptions to extract the parameters of the model, and finally a description of the computer simulation and initial conditions. See also *SI Appendix*, Table S1 for the summary of the dimensionless variables and parameters that are used in the simulations.

The final set of dimensionless dynamic equations that are solved and simulated are as follows:

Ligands and receptor levels

$$\frac{dd_i}{dt} = \beta_d + \alpha^- \left(d^M{}_i + d^N{}_i\right) - \alpha^N \beta_{N\_def} \left(\rho_N^M + \frac{N_i}{\beta_{N\_def}}\right) d_i - \left(1 + K_c n_i\right) d_i,$$

$$\frac{dd^M{}_i}{dt} = \alpha^N \beta_{N\_def} \rho_N^M d_i - \left(\alpha^- + 1 + K_t \varepsilon_N^M \left\langle n_j \right\rangle_i + K_c n_i\right) d^M{}_i,$$

$$\frac{dd^N{}_i}{dt} = \alpha^N N_i d_i - \left(\alpha^- + 1 + K_t \left\langle n_j \right\rangle_i + K_c n_i\right) d^N{}_i,$$

$$\frac{dn_i}{dt} = \beta_n - n_i - K_t \left(\varepsilon_N^M \left\langle d^M{}_j \right\rangle_i + \left\langle d^N{}_j \right\rangle_i\right) n_i - K_c \left(d_i + d^M{}_i + d^N{}_i\right) n_i.$$

Intracellular components levels

$$\frac{dE_i}{dt} = \beta_E \frac{\left[K_t \left(\varepsilon_N^M \left\langle d^M{}_j \right\rangle_i + \left\langle d^N{}_j \right\rangle_i\right) n_i\right]^{c_S}}{1 + \left[K_t \left(\varepsilon_N^M \left\langle d^M{}_j \right\rangle_i + \left\langle d^N{}_j \right\rangle_i\right) n_i\right]^{c_S}} - E_i,$$

$$\frac{dg_i}{dt} = \beta_g(r) \frac{1}{1 + \left(\frac{E_i}{T_E}\right)^{c_E}} - g_i,$$

$$\frac{dN_i}{dt} = \beta_N \frac{\left(\frac{g_i}{T_g}\right)^{c_g}}{1 + \left(\frac{g_i}{T_g}\right)^{c_g}} - N_i,$$

where

d_i, $d^M{}_i$, $d^N{}_i$, n_i, E_i, g_i, and N_i are the levels in cell i of nonubiquitylated Dl, Mib1-ubiquitylated Dl, Neur-ubiquitylated Dl, Notch, E(Spl), ac/sc, and Neur, respectively.

$\left\langle d_j \right\rangle_{i'} \left\langle d^M{}_j \right\rangle_{i'} \left\langle d^N{}_j \right\rangle_{i'}$ and $\left\langle n_j \right\rangle_i$ are the sum of the levels from cells j on the boundaries with cell i of nonubiquitylated Dl, Mib1-ubiquitylated Dl, Neur-ubiquitylated Dl, and Notch, respectively.

r is a spatial variable defining the gradient profile of ac/sc.

β_d, β_n, β_E, β_g, and β_N are the expression rates of Dl, Notch, E(Spl), ac/sc, and Neur, respectively.

β_{N_def} is the β_N in the default set of parameters (wt condition).

α^N and α^- are the rates of ubiquitylation of Dl by Neur and deubiquitylation of Mib1-or Neur-ubiquitylated Dl, respectively.

ρ_N^M is the ratio between ligand activity associated with ubiquitylation by Mib1 and the maximal ligand activity associated with ubiquitylation by Neur.

K_c and K_t are the rates for CI and trans-activation, respectively.

ε_N^M is the ratio between trans-activation of Notch from Mib1- and Neur-ubiquitylated Dl.

c_S, c_E, and c_g are hill coefficients associated with the levels of Notch activity ($[NICD, Mam, Su(H)]$ complex), E(Spl), and ac/sc, respectively.

T_E and T_g are Hill half occupation levels associated with the levels of E(Spl) and ac/sc, respectively.

The equations are solved numerically, using a standard Matlab ordinary differential equations (ODE) solver, and the solution is simulated using a custom code given in https://github.com/Udi-Binshtok/SOP_model_2021 (45).

Data, Materials, and Software Availability. Matlab ordinary differential equations solver; Code generating the simulations data have been deposited in Github (45). All other data are included in the manuscript and/or *SI Appendix*.

ACKNOWLEDGMENTS. We thank Stefan Kölzer for excellent technical assistance. The Bloomington Drosophila Stock Center (NIH P40OD018537), the Vienna Drosophila Resource Center, the Drosophila Genomics Resource Center (NIH 2P40OD010949-10A1), and the Drosophila Hybridoma Bank supplied fly stocks and reagents. The work of T.T. and T.K. are supported by the Deutsche Forschungsgemeinschaft (DFG) through Sachbeihilfe GZ: KL 1028/9-1. D.S. and T.K. are grateful for the support of the DFG via Sachbeihilfe (Middle East Grant) KL1028/13-1. U.B. is supported by the Postdoctoral Fellowships program of The Israel Academy of Sciences and Humanities.

1. C. Siebel, U. Lendahl, Notch signaling in development, tissue homeostasis, and disease. *Physiol. Rev.* **97**, 235–294 (2017).
2. S. Artavanis-Tsakonas, M. D. Rand, R. J. Lake, Notch signaling: Cell fate control and signal integration in development. *Science* **284**, 77ß-776 (1999).
3. J. F. de Celis, S. Bray, Feed-back mechanisms affecting Notch activation at the dorsoventral boundary in the Drosophila wing. *Development* **124**, 3241–3251 (1997).
4. T. Klein, K. Brennan, A. M. Martinez-Arias, An intrinsic dominant negative activity of serrate that is modulated during wing development in Drosophila. *Dev. Biol.* **189**, 123–134 (1997).
5. C. A. Micchelli, E. J. Rulifson, S. S. Blair, The function and regulation of cut expression on the wing margin of Drosophila: Notch, Wingless and a dominant negative role for Delta and Serrate. *Development* **124**, 1485–1495 (1997).
6. D. Sprinzak, S. C. Blacklow, Biophysics of Notch Signaling. *Annu. Rev. Biophys.* **50**, 157–189 (2021).
7. D. del Álamo, H. Rouault, F. Schweisguth, Mechanism and significance of cis-inhibition in Notch signalling. *Curr. Biol.* **21**, R40–R47 (2011).
8. J. L. Gomez-Skarmeta, S. Campuzano, J. Modolell, Half a century of neural prepatterning: The story of a few bristles and many genes. *Nat. Rev. Neurosci.* **4**, 587–598 (2003).
9. U. Binshtok, D. Sprinzak, Modeling the Notch response. *Adv. Exp. Med. Biol.* **1066**, 1066–1079 (2018).
10. A. Daskalaki *et al.*, Distinct intracellular motifs of Delta mediate its ubiquitylation and activation by Mindbomb1 and Neuralized. *J. Cell Biol.* **195**, 1017–1031 (2011).
11. A. L. Parks, S. S. Huppert, M. A. Muskavitch, The dynamics of neurogenic signalling underlying bristle development in Drosophila melanogaster. *Mech. Dev.* **63**, 61–74 (1997).
12. T. Troost, M. Schneider, T. Klein, A re-examination of the selection of the sensory organ precursor of the bristle sensilla of Drosophila melanogaster. *PLoS Genet.* **11**, e1004911 (2015).
13. O. Barad, D. Rosin, E. Hornstein, N. Barkai, Error minimization in lateral inhibition circuits. *Sci. Signal.* **3**, ra51 (2010).
14. P. Formosa-Jordan, M. Ibañes, Competition in notch signaling with Cis enriches cell fate decisions. *PLoS One* **9**, e95744 (2014), 10.1371/journal.pone.0095744.
15. A. Yaron, D. Sprinzak, The cis side of juxtacrine signaling: A new role in the development of the nervous system. *Trends Neurosci.* **35**, 230–239 (2011).
16. D. Sprinzak *et al.*, Cis-interactions between Notch and Delta generate mutually exclusive signalling states. *Nature* **465**, 86–90 (2010).
17. N. Berndt *et al.*, Ubiquitylation-independent activation of Notch signalling by Delta. *eLife* **6**, e27346 (2017), 10.7554/eLife.27346.
18. S. Chanet, N. Vodovar, V. Mayau, F. Schweisguth, Genome engineering-based analysis of Bearded family genes reveals both functional redundancy and a nonessential function in lateral inhibition in Drosophila. *Genetics* **182**, 1101–1108 (2009).
19. O. Shaya *et al.*, Cell-cell contact area affects notch signaling and notch-dependent patterning. *Dev. Cell* **40**, 505–511 (2017).
20. P. Cubas, J. F. de Celis, S. Campuzano, J. Modolell, Proneural clusters of achaete-scute expression and the generation of sensory organs in the Drosophila imaginal wing disc. *Genes Dev.* **5**, 996–1008 (1991).
21. P. Cubas, J. Modolell, The extramachrochaete gene provides information for sensory organ patterning. *EMBO J.* **11**, 3385 (1992).
22. I. Rodríguez, R. Hernández, J. Modolell, M. Ruiz-Gómez, Competence to develop sensory organs is temporally and spatially regulated in Drosophila epidermal primordia. *Embo J.* **9**, 3583–3592 (1990).
23. R. Fernandez-Valdivia *et al.*, Regulation of mammalian Notch signaling and embryonic development by the protein O-glucosyltransferase Rumi. *Development* **138**, 1925–1934 (2011).
24. D. Doherty, G. Feger, S. Younger-Shepherd, L. Y. Jan, Y. N. Jan, Delta is a ventral to dorsal signal complementary to Serrate, another Notch ligand. Drosophila wing formation. *Genes Dev.* **10**, 421–434 (1996).
25. R. J. Fleming *et al.*, An extracellular region of Serrate is essential for ligand-induced cis-inhibition of Notch signaling. *Development* **140**, 2039–2049 (2013).
26. M. Furriols, S. Bray, A model response element detects suppressor of hairless-dependent molecular switch. *Curr Biol.* **11**, 60–64 (2001).
27. J. P. Couso, S. A. Bishop, Arias A. Martinez, The wingless signalling pathway and the patterning of the wing margin in Drosophila. *Development* **120**, 621–636 (1994).
28. S. W. Miller, J. W. Posakony, Lateral inhibition: Two modes of non-autonomous negative autoregulation by neuralized. *PLoS Genet.* **14**, e1007528 (2017), 10.1371/journal.pgen.1007528.
29. C. Pitsoli, C. Delidakis, The interplay between DSL proteins and ubiquitin ligases in Notch signaling. *Development* **132**, 4041–4050 (2005).
30. Y. Li, N. E. Baker, The roles of cis-inactivation by Notch ligands and of neuralized during eye and bristle patterning in Drosophila. *BMC Dev. Biol.* **4**, 5 (2004).
31. L. Seugnet, P. Simpson, M. Haenlin, Transcriptional regulation of Notch and Delta: Requirement for neuroblast segregation in Drosophila. *Development* **124**, 2015–2025 (1997).
32. F. Corson, L. Couturier, H. Rouault, K. Mazouni, F. Schweisguth, Self-organized Notch dynamics generate stereotyped sensory organ patterns in Drosophila. *Science* **356**, eaai7407 (2017). 10.1126/science.aai7407.
33. M. Cohen, M. Georgiou, N. L. Stevenson, M. Miodownik, B. Baum, Dynamic filopodia transmit intermittent Delta-Notch signaling to drive pattern refinement during lateral inhibition. *Dev. Cell* **19**, 78–89 (2010).
34. H. Gerhardt *et al.*, VEGF guides angiogenic sprouting utilizing endothelial tip cell filopodia. *J. Cell Biol.* **161**, 1163–1177 (2003).
35. Sagar, F. Pröls, C. Wiegreffe, M. Scaal, Communication between distant epithelial cells by filopodia-like protrusions during embryonic development. *Development* **142**, 665–671 (2015).
36. I. Geffers *et al.*, Divergent functions and distinct localization of the Notch ligands Dll1 and Dll3 in vivo. *JCB* **178**, 465–476 (2007).
37. A. Loewer, P. Soba, K. Beyreuther, R. Paro, G. Merdes, Cell-type-specific processing of the amyloid precursor protein by Presenilin during Drosophila development. *EMBO Rep.* **4**, 405–411 (2004).
38. T. Klein, A. M. Martinez-Arias, Different spatial and temporal interactions between Notch, wingless, and vestigial specify proximal and distal pattern elements of the wing in Drosophila. *Dev. Biol.* **194**, 196–212 (1998).
39. R. Le Borgne, S. Remaud, S. Hamel, F. Schweisguth, Two distinct E3 ubiquitin ligases have complementary functions in the regulation of delta and serrate signaling in Drosophila. *PLoS Biol.* **3**, e96 (2005).
40. C. A. Micchelli, S. S. Blair, Dorsoventral restriction in wing imaginal discs requires Notch. *Nature* **401**, 473–476 (1999).
41. G. L. Boulianne, A. de la Concha, J. A. Campos-Ortega, L. Y. Jan, Y. N. Jan, The Drosophila neurogenic gene neuralized encodes a novel protein and is expressed in precursors of larval and adult neurons. *Embo J.* **12**, 2586 (1993).
42. J.-E. Gomes, M. Corado, F. Schweisguth, Van Gogh and Frizzled act redundantly in the Drosophila sensory organ precursor cell to orient its asymmetric division. *PLoS One.* **4**, e4485 (2009), 10.1371/journal.pone.0004485.
43. S. A. Speicher, U. Thomas, U. Hinz, E. Knust, The Serrate locus of Drosophila and its role in morphogenesis of the wing imaginal discs: Control of cell proliferation. *Development* **120**, 535–544 (1994).
44. J. A. Croker, S. L. Ziegenhorn, R. A. Holmgren, Regulation of the Drosophila transcription factor, Cubitus interruptus, by two conserved domains. *Dev. Biol.* **291**, 368–381 (2006).
45. Udi Binshtok, TCS model *simulation* code, *GitHub*, https://github.com/Udi-Binshtok/SOP_model_2021, September 28, 2021